Solvent-Dependent Conformation and Hydrogen-Bonding Capacity of Cyclosporin A: Evidence from Partition Coefficients and Molecular Dynamics Simulations

Nabil El Tayar,[†,§] Alan E. Mark,[‡] Philippe Vallat,[†] Roger M. Brunne,[‡] Bernard Testa,*[,†] and Wilfred F. van Gunsteren[‡]

Institut de Chimie Thérapeutique, Ecole de Pharmacie, Université de Lausanne, BEP, CH-1015 Lausanne, Switzerland, and Laboratorium Für Physikalische Chemie, ETH-Zentrum, CH-8092 Zürich, Switzerland

Received June 25, 1993[•]

The partition coefficient of cyclosprin A (CsA) was measured in octanol/water and heptane/water by centrifugal partition chromatography. By comparison with results from model compounds, it was deduced that the hydrogen-bonding capacity of CsA changed dramatically from an apolar solvent (where it is internally H-bonded) to polar solvents (where it exposes its H-bonding groups to the solvent). Molecular dynamics simulations in water and CCl_4 support the suggestion that CsA undergoes a solvent-dependent conformational changes and that the interconversion process is slow on the molecular dynamics time scale.

Introduction

An important prerequisite for understanding structure–activity relationships of bioactive compounds is a detailed knowledge of their predominant conformations in solvents comparable to biological media. Despite a decade of intensive studies using a battery of spectroscopic and theoretical techniques, the conformational behavior of cyclosporin A (CsA), an immunosuppressive cyclic undecapeptide widely used in clinical organ transplantation,[1-5] is still unresolved.[6-10] The crystal structure of CsA[6,7] and the structure of isolated CsA in apolar solvents as determined using two-dimensional NMR techniques[7,8] are similar. The basic features of the dominant conformer, as illustrated in Figure 1, are the presence of stable intramolecular H-bonds NH···O=C leading to the formation of a stable twisted β-sheet and a type II' β-turn at Sar3 and MeLeu4. In contrast to the situation in apolar solvents where a single conformer dominates, NMR spectra of CsA in polar solvents[8-10] such as DMSO, THF/LiCl and ethanol/water suggest the coexistence of various stable conformers. The solubility of CsA is not sufficient to allow the study of the conformation of uncomplexed CsA in water using NMR. For this reason a series of molecular dynamics simulations was performed by Lautz et al.[11] to investigate the effect of an aqueous environment on the structure and dynamics of CsA. The study consisted of a number of short 40-50-ps simulations starting from the crystal structure and demonstrated differences in the dynamics but provided no clear indication as to the possible existence of different conformers in water as compared to apolar solvents.

Surprisingly, recent NMR and X-ray studies[12-15] in water of CsA bound to cyclophilin, a protein that specifically binds CsA, revealed a significantly different conformation of CsA. This conformer contains no intramolecular H-bonds and exposes nearly all polar groups to the aqueous environment (Figure 1). In this context, a number of current investigations focus on whether this conformational change of CsA in aqueous solution is caused by binding interactions with cyclophilin or is simply induced by solvent effects. More recently, a conformation similar to that of CsA bound to cyclophilin has been established by crystallographic analysis of CsA bound to a Fab molecule in aqueous environment.[16] The dissimilarity of the surfaces of CsA interacting with cyclophilin and Fab molecules led Altschuh et al.[16] to suggest that the conformation of CsA observed in the bound state preexists in aqueous solution and is not induced by binding to the protein. Furthermore, kinetic studies[17] of enzyme-bound CsA and CsA–cyclophilin interactions have also indicated that water induces dramatic changes in the conformation of CsA before binding to the enzyme. CsA was shown to be a slow-binding inhibitor of the peptidylprolyl *cis–trans* isomerase cyclophilin. Indeed, both the initial inhibitory activity and the subsequent time-dependent inhibition are sensitive to the solvent system (DMSO, THF, ···, etc.) in which CsA is dissolved prior to the assay. This behavior led Rich[18] to introduce the concept of "hydrophobic collapse" as a tool for peptidomimetics design.

The purpose of this study is to attempt to verify these hypotheses by extracting structural information derived (a) from the experimental investigation of the partitioning behavior of CsA in various solvent systems and (b) from a series of molecular dynamics simulations. The partition coefficient (expressed as log P) is a physicochemical property which describes a partitioning equilibrium of solute molecules between water and an organic solvent, and as such is of particular significance in drug design because it reflects the combined effects of intramolecular interactions and intermolecular forces between the solute and its environment.[19-21] A recent evaluation of forces governing the partitioning of solutes in various solvent systems has clearly demonstrated that the octanol/water and heptane/water solvent systems produce significantly different balances of intermolecular forces, in particular for the H-bonds.[22] For example, the H-bond donor acidity of solutes is completely balanced in octanol/water (both octanol and water having similar H-bond acceptor basicity), and its net contribution to the partitioning equilibrium in this system is close to zero. In contrast, in heptane/water, this term contributes significantly to the partitioning process. Unlike heptane, octanol is known to break intromolecular H-bonds by virtue of its polarity and its high water content at saturation. Thus, the $\Delta(\log P_{oct\ hep})$ parameter (i.e. $\log P_{oct} - \log P_{hep}$) can provide a quantitative

† Université de Lausanne.
‡ ETH-Zentrum.
§ Present address: Ares Serono, Chemin des Mines 15bis, CH-1202 Geneva, Switzerland.
• Abstract published in *Advance ACS Abstracts*, October 15, 1993.

0022-2623/93/1836-3757$04.00/0

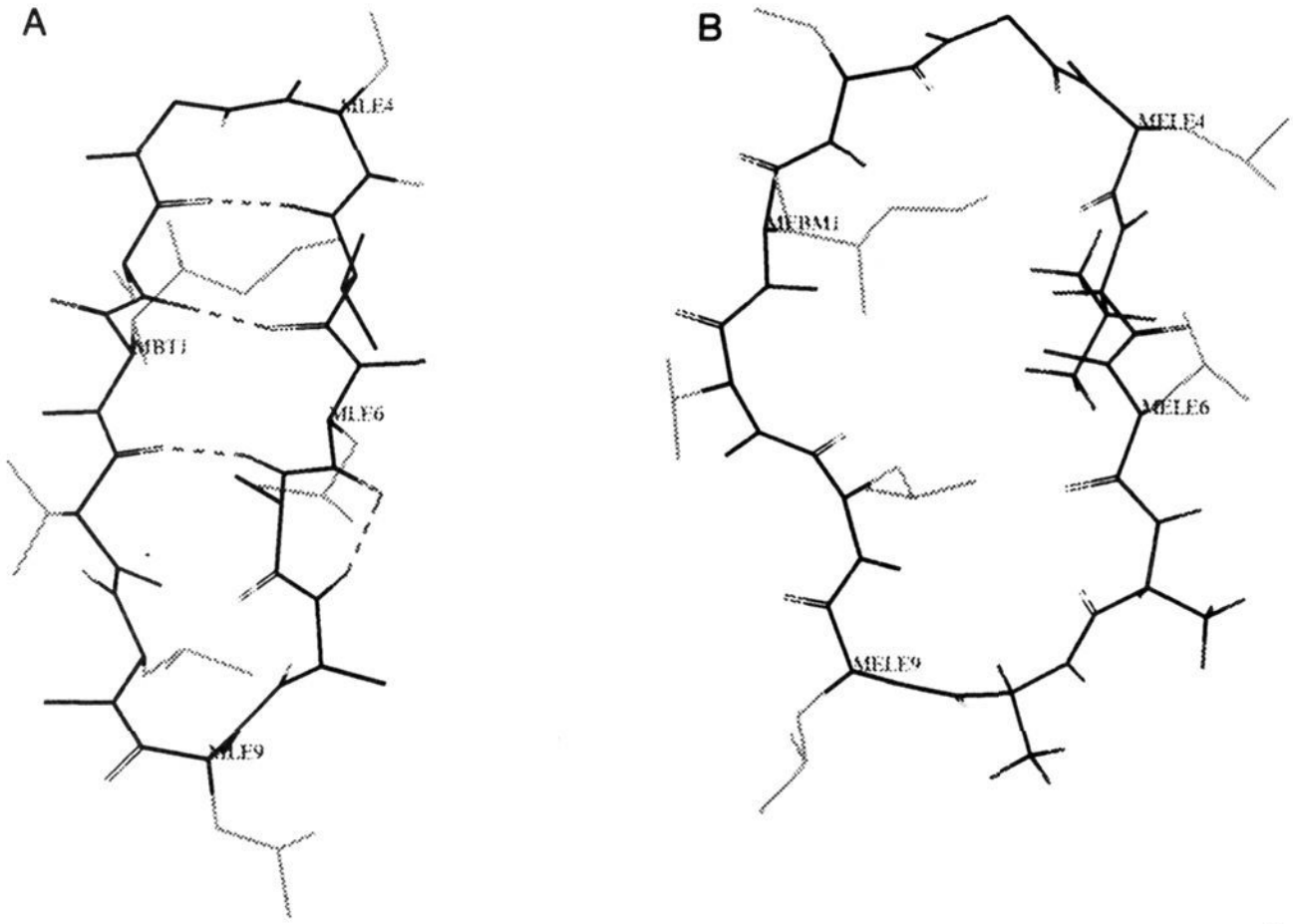

Figure 1. Environment-dependent conformation of CsA. (A) X-ray structure of CsA;[6,7] (B) NMR structure of CsA bound to cyclophilin in water.[2] The internal H-bonds are indicated by broken lines.

Table I. Partition Coefficients (log P) and H-Bond Donor Acidity [$\Delta(\log P_{oct-hep})$] of CsA and Some Model Solutes

solute	log P_{oct}	log P_{hep}	$\Delta(\log P_{oct-hep})$	CLOGP[a]
CsA	2.92	1.40	1.52	14.0
cyclo(Phe-Phe)	1.59	<−3.0	>4.5	2.86
cyclo(Trp-Tyr)	1.05	<−3.0	>4.1	2.19
benzamide	0.65	−2.45[b]	3.10	0.66
o-fluorobenzamide	0.64[b]	−1.47	2.11	0.50
p-fluorobenzamide	0.96	−2.34	3.25	1.00
acetanilide	1.16[b]	−1.54	2.70	1.16
o-fluoroacetanilide	0.96[b]	−0.69	1.65	0.96
p-fluoroacetanilide	1.47[b]	−1.57	3.04	1.61
phenol	1.46[b]	−0.82	2.22	1.48
o-nitrophenol	1.68	1.04[b]	0.64	1.85
p-nitrophenol	1.77	−2.11	3.88	1.85

[a] Calculated octanol/water partition coefficients using the CLOGP algorithm.[26] [b] Experimental log P values taken from the literature.[26]

estimate of the H-bond donor acidity of a given solute and also shed light on the solvent accessibility of its H-bonding groups.[22,23] Hence, a partitioning study of solutes in different solvent systems with different polarity should yield information on the shift in conformation populations upon accompanying change in solvent environment.

In an effort to better understand the effect of the polarity of the solvent on the conformation of CsA, we measured the partition coefficients of this peptide and some model compounds in two solvent systems of different polarity, namely 1-octanol/water buffer and *n*-heptane/water buffer using centrifugal partition chromatography (CPC).[24,25] In order to relate the effect of the solvent to changes at a molecular level, a molecular dynamics simulation study in water and CCl_4 was undertaken. The simulations extend considerably those performed previously by Lautz et al.[11] and were also used to investigate differences in the interaction of the crystal conformation of CsA, and of the cyclophilin bound conformation, with water and CCl_4.

Results and Discussion

Partitioning Behavior of Cyclosporin A. Table I shows the partition coefficient values of CsA and other solutes in octanol/aqueous buffer and heptane/aqueous buffer solvent systems. The estimated log P_{oct} values, as calculated by the MedChem program CLOGP,[26] and the $\Delta(\log P_{oct-hep})$ values are also reported in Table I. A good correlation ($r^2 = 0.98$) is obtained between the observed and estimated log P_{oct} values for all compounds except CsA and the two cyclodipeptides. For CsA, a very high and unrealistic value (CLOGP = 14) was estimated. Despite its usefulness, the CLOGP algorithm thus has difficulties with complex structures. In fact, the CLOGP algorithm is based only on 2D structures and neglects the solvent inaccessibility of some fragments while exaggerating the correction factors for polar proximity effects. This is particularly true when a large nonpolar group is flanked by two polar groups as is indeed the case for the two cyclodipeptides and CsA. Recent progress toward the development of a conformation-dependent lipophilicity index appears promising and should alleviate these problems.[27,28]

The log P_{hep} value (1.40) of CsA is very high compared to that of cyclo(Phe-Phe) despite the fact that CsA contains four strong H-bond donor CONH groups and one hydroxyl group. The $\Delta(\log P_{oct-hep})$ value of the flexible CsA (1.52) is also very low compared to the rigid cyclo(Phe-Phe) (>4.5). It has been shown that the $\Delta(\log P_{oct-hep})$ value of an amide group (e.g. in acetanilide or benzamide) and a hydroxyl group (e.g. in phenol) are higher than 2.7 and 2, respectively. However, when the H-bond donor group is involved in an internal H-bond, its H-bond donor acidity decreases dramatically, as evidenced by the lower $\Delta(\log P_{oct-hep})$ values of *o*-fluorobenzamide, *o*-fluoroacetanilide, and *o*-nitrophenol compared to their *para* isomers (Table I). These internal H-bonds are known to be strongly favored in media of low polarity such as *n*-heptane. This effect explains the higher than expected log P_{hep} value of solutes able to form an internal H-bond. In addition, one should keep in mind that the relatively high polarity of water-saturated octanol (at saturation octanol contains 4% of water) diminishes the probability of intramolecular

Table II. Root Mean Square (RMS) Positional Deviations[a,b] between the X-ray (XRAY) or Cyclophilin (CyPB) Derived Structures of CsA and Average Structure from 150- to 200-ps Simulations in H_2O and CCl_4

	XRAY	CyPB	XRAYH_2O	CyPBH_2O	XRAYCCl_4	CyPBCCl_4
XRAY	-	0.31	0.12(0.10)	0.27	0.06	0.27
CyPB	0.47	-	0.26(0.27)	0.10	0.30	0.11
XRAYH_2O	0.14(0.14)[c]	0.43(0.44)	-	0.22(0.23)	0.09(0.08)	0.22(0.23)
CyPBH_2O	0.46	0.17	0.42(0.43)	-	0.27	0.04
XRAYCCl_4	0.11	0.47	0.10(0.10)	0.45	-	0.26
CyPBCCl_4	0.45	0.17	0.41(0.42)	0.08	0.44	-

[a] Deviations are given in nanometers and calculated after performing a least-squares rotational and translational fit on all Cα atoms. [b] RMS deviations between Cα atoms are given in the upper right section while deviations between all atoms are given in the lower left section. [c] Values in parentheses are the RMS deviations using the average from 350 to 400 ps.

Table III. Average Energies of Interactions (in kJ mol^{-1}) of Various Conformations of CsA in H_2O and CCl_4

interactions[a]	XRAYH_2O	CyPBH_2O	XRAYCCl_4	CyPBCCl_4
solvent–solvent–ELE[b]	-35069(±213)[d]	-35065(±231)	-	-
solvent–solvent–LJ[c]	-5254(±141)	-5250(±145)	-11957(±101)	-11956(±98)
CsA–solvent–ELE	-242(±42)	-323(±34)	-	-
CsA–solvent–LJ	-483(±24)	-527(±26)	-430(±17)	-457(±19)
CsA–CsA–ELE	-60(±12)	-36(±7)	-73(±10)	-51(±9)
CsA–CsA–LJ	-36(±24)	-9(±24)	-61(±25)	-33(±27)
angle energy of CsA	193(±20)	201(±22)	188(±19)	203(±19)
dihedral energy of CsA	79(±18)	79(±16)	82(±18)	87(±17)
total intra-CsA	176(±38)	235(±37)	136(±38)	206(±38)
total CsA	-548(±61)	-615(±56)	-294(±42)	-251(±41)

[a] The energy of interactions represent an estimate of the enthalpic term. [b] Electrostatic interaction term. [c] Lennard–Jones interaction term. [d] The standard deviations of the averages in the 50–200-ps range are given in parentheses.

H-bonds. This is evidenced by the lower log P_{oct} value of the *ortho* isomers in Table I compared to the *para* isomers. For cyclodipeptides, the two CONH groups cannot form an internal H-bond, whatever the solvent polarity, due to the rigidity of the molecule. This leads to $\Delta(\log P_{oct\text{-}hep})$ values higher than 4.5 as exemplified by cyclo(Phe-Phe).

Unlike cyclodipeptides, CsA has a flexible structure which can adopt various conformations depending on the solvent polarity. As previously discussed, CsA in apolar solvents adopts a folded conformation stabilized by intramolecular H-bonds between the strong H-bond donor amide groups and the strong H-bond acceptor carbonyl groups. In contrast, in polar solvents, CsA can adopt more open conformations which expose its polar groups to the polar solvent following cleavage of the internal H-bonds. Thus, large flexible molecules can adapt their conformation in order to expose to the environment those groups that can best interact with it (a "chameleonic" behavior).[29] Therefore, the lower than expected $\Delta(\log P_{oct\text{-}hep})$ value of CsA, despite the fact it contains four strong H-bond donor amide groups and one hydroxyl group, might indicate a conformational shift from predominantly "closed", internally H-bonded conformers in heptane to predominantly "open" conformers in octanol.

A number of experimental papers[30-33] have investigated the fundamental issue of conformational shift upon change in solvent environment. The large body of evidence relating to environmentally induced conformational shifts has been used to design molecules which will change from a very broad conformational distribution in aqueous solution to a prespecified helical structure upon transfer to a lipid environment. For example,[33] the dependence of the chemical shifts of the amide protons of the cyclohexapeptide cyclo(Asn-Pro-Ala-Leu-Pro-Gly) with increasing DMSO-d_6 content in $CDCl_3$/DMSO-d_6 mixtures was attributed to a cleavage of the internal H-bonds leading to conformations with a higher number of exposed amide protons to the good H-bond acceptor DMSO-d_6.

Our partitioning results are also in line with the speculations of Altschuh et al.[16] and Rich[17] that the conformation of CsA observed in the bound state might preexist in aqueous solution and is not induced by binding to the protein.

Molecular Dynamics Simulations. Table II shows root mean square (RMS) positional deviations between the X-ray and cyclophilin-bound structures of CsA simulated in water and in CCl_4 as well as the RMS deviations to the respective starting structures. The structures derived from the simulations correspond to trajectory averages from 150 to 200 ps. From Table II it can be seen that irrespective of the solvent both conformations remain significantly closer to their respective starting structures than to the starting structure of the other conformer during the 200-ps initial simulations. No significant change was observed when the simulation of the X-ray structure in water was extended by a further 200 ps. Interconversion of the two conformers would provide the most convincing evidence that CsA adopts different conformations depending on the polarity of the solvent. It is, however, not surprising that such interconversion was not observed during the simulations. Recent NMR studies have suggested the presence of multiple conformers in CD_3OD/D_2O and $CDCl_3$/CD_3OD mixtures.[34,35] These studies indicate that the interconversion is slow on the NMR time scale and therefore well beyond the reach of the current computational means. Nevertheless, the simulations provide a body of evidence to suggest that the cyclophilin-bound conformation is in fact comparatively more stable in water than the X-ray conformation.

Table III lists interaction energies averaged from 50 to 200 ps for each of the four simulations. The energy values have been grouped on the basis of force-field interaction terms and separated into solute and solvent components. Considering just the intrasolute terms, i.e., Lennard–Jones, electrostatic, and bonded terms between CsA atoms, it can be seen that the CsA conformation observed in the crystal is enthalpically favored over the CyPB conformation. In both solvents the simulation started from the CyPB conformation has a higher internal energy than that started from the crystal structure. The X-ray conforma-

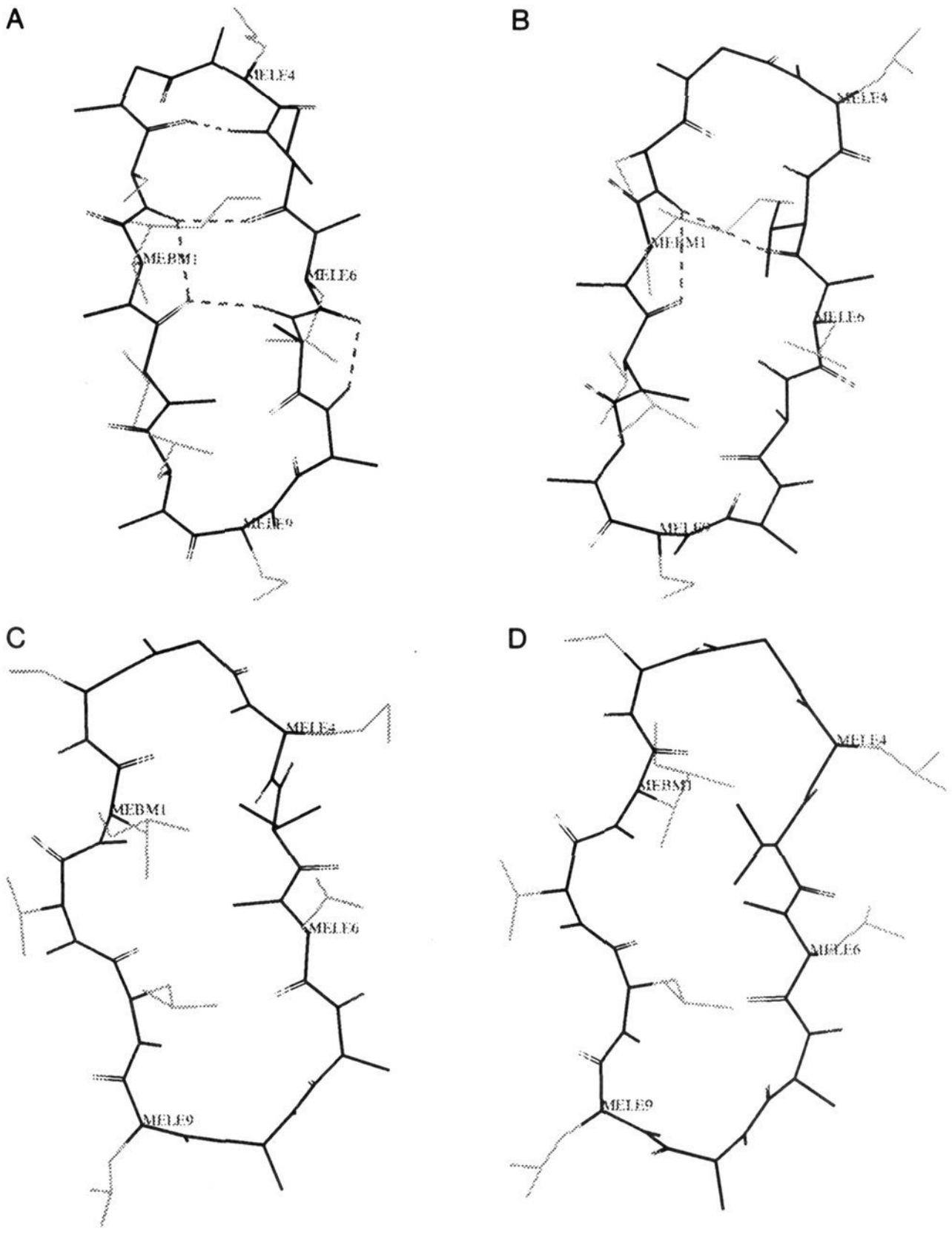

Figure 2. Average structures of CsA over 150–200-ps trajectories. (A) X-ray structure in CCl_4 ($XRAYCCl_4$); (B) X-ray structure in water ($XRAYH_2O$); (C) Cyclophilin-bound structure in CCl_4 ($CyPBCCl_4$); (D) Cyclophilin-bound structure in water ($CyPBH_2O$). The internal H-bonds are indicated by broken lines.

tion in CCl_4 which shows the smallest deviation from the starting structure has an intramolecular potential energy of 136 kJ mol^{-1}. The CyPB structure in water has for comparison an intramolecular potential energy of 235 kJ mol^{-1}. When comparing energies between simulations it should be noted that different cutoff criteria were used in water and CCl_4. Due to the difference in the size of the solvent molecule, a cutoff of 1.3 nm was used for the Lennard–Jones interactions in the simulations in CCl_4 as opposed to a cutoff of 0.8 nm in water. Increasing the cutoff from 0.8 to 1.3 nm lowers the internal Lennard–Jones energy by approximately 10 kJ mol^{-1}. The cutoff for the electrostatic interactions was 1.3 and 1.2 nm for the simulations in CCl_4 and water, respectively. The effect of this difference would be to lower the internal electrostatic energy by 2–5 kJ mol^{-1}. Thus, even after correcting for the effects of the different cutoff criteria the difference in the internal contribution to the total energy is over 80 kJ mol^{-1}. The sum of all interactions involving CsA is, however, dominated by interactions to solvent in each of the systems. In both solvents the CyPB conformation yields energetically more favorable interactions to the solvent than the X-ray conformation. In CCl_4 this difference is less than the difference in stabilization between the two conformers. The X-ray conformation optimizes internal energetic terms at the expense of interactions to CCl_4. The net difference between the X-ray and CyPB conformations in CCl_4 is approximately 40 kJ mol^{-1} in favor of the X-ray conformation. In water the opposite effect is observed. The interaction between CsA in the CyPB conformation and water is stronger by 125 kJ mol^{-1} than the interaction between the X-ray-derived conformation and water. The X-ray structure adapts to an aqueous environment by adopting a more internally strained conformation in order to optimize contacts with the solvent. The net effect is that the CyPB structure is enthalpically more stable in water by approximately 60 kJ mol^{-1}. Thus, during the simulations there is a slight tendency for the X-ray structure to converge closer to the initial CyPB structure in H_2O than in CCl_4 and for the

Table IV. Stability of the Internal H-Bonds Found in H_2O and CCl_4 in the Simulations Starting from the X-ray Structure

	occupancies, % donor → acceptor[a]					
conformation[b]	Abu2-Val5	Abu2-MeVal11	Val5-Abu2	Val5-Sar3	Ala7-MeVal11	Ala8-MeLeu6
Simulations in H_2O						
1–50 ps	33	14	70	<5	48	12
51–100 ps	29	15	80	<5	62	6
101–150 ps	43	12	70	<5	55	13
151–200 ps	10	7	58	8	–	–
201–250 ps	40	<5	83	<5	43	15
251–300 ps	33	<5	49	13	39	14
301–350 ps	20	<5	67	<5	11	28
351–400 ps	17	7	21	–	10	8
Simulations in CCl_4						
1–50 ps	55	9	70	7	66	67
51–100 ps	35	14	66	9	53	54
101–150 ps	42	5	62	11	58	57
151–200 ps	45	10	68	8	57	58

[a] The donor and acceptor groups are the proton and carbonyl of the amide group, respectively. [b] Average percent occupancy over 50-ps trajectories.

Table V. Intermolecular H-Bonds between the X-ray Conformation of CsA Acting as Donor and Water Acting as Acceptor

	occupancies, %			
conformation	H[a] Abu2	H Val5	H Ala7	H Ala8
1–50 ps	9	–	<5	60
51–100 ps	<5[b]	–	–	78
101–150 ps	<5	–	31	65
151–200 ps	13	–	94	81
201–250 ps	15	<5	17	54
251–300 ps	9	<5	<5	56
301–350 ps	31	19	66	40
351–400 ps	5	73	<5	67

[a] This refers to the polar hydrogen of the amide group. [b] Occupancies of <5% are not considered significant.

CyPB to converge toward the X-ray structure in CCl_4 (see Table II). However, it should be noted that, although close, the X-ray structure of CsA (Figure 1A) is not identical with the average structure in CCl_4 as determined by NMR and that the CyPB structure (Figure 1B) is unlikely to represent the average conformation in aqueous solution. This fact is partly reflected in the observation that the average $XRAYH_2O$ structure is closer to the average $CyPBH_2O$ structure than to the initial CyPB structure (Table II).

H-Bond Pattern. Although there is no explicit hydrogen bonding term in the GROMOS force field, the effect of hydrogen bonds is mimicked by a combination of Lennard-Jones and electrostatic terms. This has been shown to be very effective in the prediction of H-bonding patterns.[42] The X-ray structure of CsA consists predominantly of β-pleated sheets, all nonmethylated backbone nitrogens forming intramolecular H-bonds with carbonyl groups. In contrast, the structure of CyPB–CsA is "open" and lacks internal H-bonds, the backbone amide hydrogen and carbonyl groups being available for H-bonding with the environment. During the simulation of the X-ray structure of CCl_4, the basic hydrogen pattern observed in the crystal was maintained. In contrast, the simulation in water revealed a progressive loss of the internal H-bonds in favor of interactions with water. The H-bonds between backbone amide and carbonyl groups as percent occupancies are given in Table IV for the simulations starting from the X-ray structure in water and CCl_4. Values are given for 50-ps windows. A H-bond is considered to exist if the proton–acceptor distance does not exceed 0.25 nm and the donor–proton–acceptor angle is larger than 135°. An inspection of Table IV reveals that the H-bond from Ala8 to MeLeu6 is lost early in the simulation in water. Internal H-bonds with Ala7 and Ala8 as donors show large fluctuations and were not observed in the period 151–200 ps. The H-bond from Val5 to Abu2 appears the most stable in water though the percentage of occupancy for this H-bond falls to only 21% frm 351 to 400 ps. In contrast, the internal backbone H-bonds remain effectively constant in the simulation starting from the X-ray structure in CCl_4. The internal H-bonds lost in the simulation in water were replaced by interactions to solvent. Tables V and VI show respectively the percentage occupancy of H-bonds from the backbone amide protons to water and from water to the backbone carbonyl groups. In Table V it can be seen that for the amide protons of Val5, Ala7, and Ala8 there is, in general, a strong correspondence between the loss of the internal H-bond and the formation of interaction with water. Only the amide protons and carbonyl oxygens of Val5 and Abu2 appear to be significantly protected from the solvent. During the simulations starting from the CyPB structure in both water and CCl_4 no internal H-bonds with an occupancy of more than 5% were observed.

Interconversion of X-ray and CyPB Conformers. Table III suggests that the CyPB conformer is energetically more stable in water than the X-ray conformer. As a thermodynamic property the relative stability of the two conformers is determined by the difference in their respective free energies. The difference in free energy between two closely related states of a system can be determined during a molecular dynamics simulation by calculating the work necessary to go from one state to the other via a reversible path.[36] Before free energy calculations can be attempted it is necessary to define a simple pathway by which the interconversion of the two conformers can be achieved. While it has been shown to perform the interconversion by forcing all of these dihedral angles simultaneously,[37] determination of the associated free energy would not be practical. In this study, the largest and most important difference between the two conformers is the dihedral angle ω_9 of the MeLeu9–MeLeu10 peptide bond. The force-field parameters used in the simulations effectively prevent isomerization of peptide bonds. This may have prevented the interconversion of the conformers during the simulations. To investigate whether the *cis–trans* isomerization of the ω_9 angle effectively determines the interconversion of the two conformers, a dihedral angle restraining potential with a force constant of 2500 kJ mol^{-1} rad^{-2} was applied to this dihedral angle in the simulation starting from the X-ray structure in water after 200-ps equilibration. This force constant was sufficient to force the transition from *cis* to *trans* within 1 ps. The transition of the ω_9 angle was accompanied by a transition of the ψ_9 angle leaving the overall backbone conformation largely unchanged. It is clear that forcing a single dihedral is not sufficient to achieve a rapid interconversion of the conformers. Combinations of dihedral angles were then investigated. Two additional backbone dihedral angles ψ_4 and ψ_6 were identified which adopt significantly different values between the CyPB and the X-ray structures and which were not observed to make spontaneous transitions during the simulations in water nor during preliminary simulations performed in vacuum (results not

Table VI. Intermolecular H-Bonds between the X-ray Conformation of CsA Acting as Acceptor and Water Acting as Donor

	occupancies, %[a]										
conformation	C=O MeBmt1	C=O Abu2	C=O Sar3	C=O MeLeu4	C=O Val5	C=O MeLeu6	C=O Ala7	C=O Ala8	C=O MeLeu9	C=O MeLeu10	C=O MeVal11
1-50 ps	87	31	71	105	11	78	73	62	77	91	30
51-100 ps	110	25	56	97	10	78	65	78	93	72	15
101-150 ps	106	38	67	117	11	88	89	68	76	80	27
151-200 ps	113	14	66	125	5	125	76	73	86	92	93
201-250 ps	90	8	76	104	13	93	60	74	86	84	61
251-300 ps	106	31	70	111	7	86	73	83	77	91	32
301-350 ps	106	27	82	113	55	75	78	70	85	76	53
351-400 ps	99	59	83	114	28	91	76	79	90	74	13

[a] Occupancies larger than 100% indicate multiple H-bonds.

shown). Each of the possible combinations using these dihedral angles (ψ_4, ψ_6, and ω_9) to force the interconversion was investigated. A combination of restraining all the three dihedral angles to the average values observed in the simulation of CyPB conformer in water resulted in the loss of all internal H-bonds and the formation of a novel conformer. This conformer did not spontaneously revert to the starting XRAYH_2O conformation upon removal of the restraining potential. The RMS deviation of this new conformer to the average from 150 to 200 ps of the simulation starting from the CyPB conformer in water is 0.40 nm for all atoms and 0.20 nm for Cα atoms. This is only marginally closer to the target structure than the average from the simulations in water starting from the X-ray structure in which no restraining potentials were used. Thus, forcing the transition of ω_9, or ω_9 in conjunction with ψ_4 and/or ψ_6, does not result in the rapid interconversion between the X-ray conformation and the CyPB conformation during the simulation. To mimic the transition, it appears that it would be necessary to force the transition of several dihedral angles in a concerted manner. The need for such a concerted transition would explain the slow rate of interconversion suggested by NMR studies.

Conclusion

The structural information derived from both partitioning and simulation studies provides evidence of a conformational change of CsA in polar and apolar media. These results are consistent with more recent NMR studies[14,38] of a water-soluble CsA derivative ([D-diaminobutyric acid]CsA) which indicate the presence of several different slowly interconverting conformations in aqueous solution. These results are also consistent with kinetic studies that support a time-dependent inhibition of the isomerase activity of cyclophilin by CsA.[17]

The ability to investigate peptide conformation by interpreting solvent-dependent partition coefficients represents a novel, facile methodology that should find wide applicability.

Experimental Section

Materials. Cyclosporin A was of pharmaceutical grade. Cyclodipeptides, fluorobenzamides, and nitrophenols were purchased from Fluka (Buchs, Switzerland) or Sigma (St. Louis, MO) and were of >99% purity. 3-Morpholinopropanesulfonic acid (MPS, >99% purity) was from Merck (Darmstadt, Germany), and 1-octanol and *n*-heptane (purum, ~98%) from Fluka. All compounds were used without further treatment.

Measurements of Partition Coefficients. The partition coefficients in 1-octanol/water and *n*-heptane/water systems were measured at pH 7.4 and 21 ± 1 °C by horizontal flow-through centrifugal partition chromatography using a coil planet type centrifuge (Pharma-Tech Research Corp., Baltimore, MD). The design principle of the instrument has been described elsewhere.[24,25] Two sets of three columns of PTFE tubing (3.00-mm i.d., 3.94-mm o.d.) and (0.85-mm i.d., 1.25-mm o.d.) were used. The total volume capacity of each set was 350 and 39.5 mL, respectively. A Kontron Model 420 HPLC pump was used to propel the solvent, and peaks were detected with a Kontron (Zürich, Switzerland) Model 432 UV/Vis detector coupled with a Hewlett-Packard 3392A integrator. A flowmeter from Deeside Industrial Estate (Queensferry, UK) was used for precise measurement of flow rates. A preliminary measurement of *n*-heptane/aqueous buffer partition coefficient of CsA was done using the shake-flask method. A log *P* value of 1.15 ± 0.05 was obtained.

Computational Procedure. A series of four simulations was performed to investigate the relative stability of the crystal conformation of CsA as compared to the cyclophilin-bound conformation in water and in the aprotic solvent carbon tetrachloride (CCl_4). CCl_4 was chosen as the apolar solvent because it can be effectively modeled as a single united atom, thus greatly reducing the computational cost. In addition, simulations of CsA in CCl_4 have been shown to closely reproduce NMR data obtained in $CHCl_3$. All simulations and analyses were performed using the GROMOS package of programs with the standard GROMOS force field.[39,40] In this force field nonpolar hydrogen atoms are treated as united atoms together with the heavy atoms to which they are attached. The polar hydrogen atoms are treated explicitly and experience Coloumbic but no Lennard-Jones interactions. Throughout the simulations bond lengths were constrained to equilibrium values using the SHAKE algorithm.[41] This permitted a time step of 2 fs to be used. In the case of water simulations, nonbonded interactions were treated using a twin-range method in which short-range electrostatic and Lennard-Jones interactions (<0.8 nm) were updated every time step while longer range electrostatic interactions (<1.2 nm) were updated only every 20 fs. For simulations performed in CCl_4, a single cutoff of 1.3 nm was used for all nonbonded interactions and updated every step. The water was modeled using the simple point charge (SPC) model.[42] CCl_4 was treated as an united atom with the chlorine atoms incorporated into the carbon atoms. The CCl_4 molecules carried no partial charges. The parameters for the Lennard-Jones interactions [$C_{12}^{1/2} = 75.45 \times 10^{-3}$ (kJ mol^{-1} nm^{12})$^{1/2}$ and $C_6^{1/2} = 0.5155$ (kJ mol^{-1} nm^6)$^{1/2}$] were taken from Rebertus et al.[43] The following combination rules were used to obtain interactions between the solute and solvent atoms $C_{12}(i,j) = [C_{12}(i)C_{12}(j)]^{1/2}$ and $C_6(i,j) = [C_6(i)C_6(j)]^{1/2}$.

Two different starting geometries of CsA were used. The first was derived from the X-ray crystallographic structure of isolated CsA.[6,7] The second from the NMR cyclophilin-bound structure of CsA.[12] All simulations were performed using periodic boundary conditions in a truncated octahedron box. The starting configurations of the system were generated as follows. For the MD simulations starting from the X-ray structure in water, one molecule of CsA was placed in the center of the box with a long axis of 3.603 24 nm. This box was filled with 729 water molecules, using a minimum distance of 0.23 nm between any non-hydrogen solute and solvent atom. The same procedure was applied to the cyclophilin-bound structure, resulting in a box with a long axis of 3.606 94 nm containing also 729 water molecules. In CCl_4, a minimum distance of 0.39 nm was used. The X-ray structure was placed in a box with long axis of 6.299 84 nm and filled with

729 CCl_4 molecules and the cyclophilin-bound structure was placed in a box with long axis of 6.256 94 nm and filled with 730 CCl_4 molecules.

Molecular Dynamics Protocol. Before starting the dynamics simulations, the internal strain of each system was relaxed by performing two cycles of steepest descent energy minimization each of 50 steps. During the first cycle the CsA molecule was harmonically restrained to its original conformation using a force constant of 9000 kJ mol^{-1} nm^{-2}. Only the solvent molecules were allowed to move in order to eliminate remaining close contacts and unfavorable geometric strains in the system. In the second cycle the whole system was allowed to move. During the simulations, the temperature and pressure of the systems were held constant by weakly coupling the system to an external bath.[44] The reference temperature of the bath was set at 300 K with a relaxation time of 0.01 ps for the first 5 ps and 0.1 ps thereafter. The reference pressure was 1 atm with a relaxation time of 0.05 before and 0.5 ps after the first 5 ps. During the first 5 ps of the simulations the CsA molecule was harmonically restrained to its original conformation with a force constant of 9000 kJ mol^{-1} nm^{-2}, allowing the solvent molecules to further equilibrate. Initially each system was simulated for 200 ps and it is during this period that comparative analyses were performed. The simulations of the X-ray structure in water was, however, extended to 400 ps. The simulations of the X-ray and cyclophilin-bound structures in water will be named $XRAYH_2O$ and $CyPBH_2O$, and the simulations in CCl_4 will be referred to as $XRAYCCl_4$ and $CyPBCCl_4$, respectively.

Acknowledgment. The authors are indebted to Prof. K. Wüthrich (Zürich) for the internal coordinates of cyclophilin-bound CsA. B.T. and N.E.T. are also indebted to the Swiss National Science Foundation for support.

References

(1) Rûegger, V. A.; Kuhn, M. Lichti, H.; Loosli, H.-R.; Huguenin, R.; Quiquerez, C.; von Wartburg, A. *Helv. Chim. Acta* **1976**, *59*, 1075–1092.
(2) Calne, R. Y.; White, D. J. G.; Thiru, S.; Evans, D. B.; McMaster, P.; Craddock, G. N.; Pentlow, D. B.; Rolles, K. Cyclosporin A in patients receiving renal allografts from cadaver donors. *Lancet* **1978**, No. 2, 1323–1325.
(3) Borel, J. F. The cyclosporins. *Transplant. Proc.* **1989**, *21*, 810–815.
(4) Wenger, R. M. Pharmacology of cyclosporin (Sandimmune) II. Chemistry. *Pharmacol. Rev.* **1989**, *41*, 243–247.
(5) Wenger, R. M. Cyclosporine and analogues: structural requirements for immunosuppressive activity. *Transplant. Proc.* **1986**, *28*, 213–218.
(6) Petcher, T. J.; Weber, H.-P.; Rûegger, A. Crystal and molecular structure of an iodo-derivative of the cyclic undecapeptide cyclosporin A. *Helv. Chim. Acta* **1976**, *59*, 1480–1487.
(7) Loosli, H.-R.; Kessler, H.; Oschkinat, H.; Weber, H.-P.; Petcher, T. J.; Widmer, A. The conformation of cyclosporin A in the crystal and in solution. *Helv. Chim. Acta* **1985** *68*, 682–704.
(8) Kessler, H.; Loosli, H. R.; Oschkinat, H. Assignment of the ^1H-, ^{13}C- and ^{15}N-NMR spectra of cyclosporin A in $CDCl_3$ and C_6D_6 by a combination of homo- and heteronuclear two-dimensional techniques. *Helv. Chim. Acta* **1985**, *68*, 661–681.
(9) Kessler, H.; Gehrke, M.; Lautz, J.; Kŏck, M.; Seebach, D.; Thaler, A. *Complexation* and medium effects on the conformation of cyclosporin A studied by NMR spectroscopy and molecular dynamics calculations. *Biochem. Pharmacol.* **1990**, *40*, 169–173.
(10) Vine, W.; Bowers, L. D. Cyclosporine: structure, pharmacokinetics, and therapeutic drug monitoring. *CRC Crit. Rev. Lab. Sci.* **1987**, *25*, 275–311.
(11) Lautz, J.; Kessler, H. van Gunsteren, W. F.; Weber, H.-P.; Wenger, R. M. On the dependence of molecular conformation on the type of solvent environment: A molecular dynamics study of cyclosporin A. *Biopolymers* **1990**, *29*, 1669–1687.
(12) Weber, C.; Wider, G.; von Freyberg, B.; Traber, R.; Braun, W.; Widmer, H.; Wûthrich, K. The NMR structure of cyclosporin A bound to cyclophilin in aqueous solution. *Biochemistry* **1991**, *30*, 6563–6574.
(13) Fesik, S. W.; Gampe, R. T.; Eaton, H. L.; Gemmecker, G.; Olejniczak, E. T.; Neri, P.; Holzman, T. F.; Egan, D. A.; Edalji, R.; Simmer, R.; Helfrich, R.; Hochlowski, J.; Jackson, M. NMR studies of [U-^{13}C]-cyclosporin A bound to cyclophilin: Bound conformation and portions of cyclosporin involved in binding. *Biochemistry* **1991**, *30*, 6574–6583.
(14) Kallen, J.; Spitzfaden, C.; Zurini, M. G. M.; Wider, G.; Widmer, H.; Wûthrich, K.; Walkinshaw, M. D. Structure of human cyclophilin and its binding site for cyclosporin A determined by X-ray crystallography and NMR spectroscopy. *Nature* **1991**, *353*, 276–279.
(15) Fesik, S. W.; Neri P.; Meadows, R.; Olejniczak, E. T.; Gemmecker, G. A model of the cyclophilin/cyclosporin A complex from NMR and X-ray data suggests that cyclosporin A binds as a transition-state analogue. *J. Am. Chem. Soc.* **1992**, *114*, 3165–3166.
(16) Altschuh, D.; Vix, O.; Rees, B.; Thierry, J.-C. A conformation of cyclosporin A in aqueous environment revealed by the X-ray structure of a cyclosporin-Fab complex. *Science* **1992**, *256*, 92–94.
(17) Kofron, J. L.; Kuzmic, P.; Kishore, V. Gemmecker, G.; Fesik, S. W.; Rich, D. H. *J.* Lithium chloride perturbation of cis-trans peptide bond equilibria: Effect on conformational equilibria in cyclosporin A and on time-dependent inhibition of cyclophilin. *J. Am. Chem. Soc.* **1992**, *114*, 2670–2675.
(18) Rich, D. H. Effect of hydrophobic collapse on enzyme-inhibitor interactions. Implications for the design of peptidomimetics. In *Perspectives in Medicinal Chemistry*; Testa, B., Kyburz, E., Fuhrer, W., Giger, R., Eds.; Verlag Helvetica Chimica Acta: Basel, 1993; pp 15–25.
(19) Hansch, C.; Leo, A. *Substituent Constants for Correlation Analysis in Chemistry and Biology*; Wiley: New York, 1979.
(20) van de Waterbeemd, H.; Testa, B. The parametrization of lipophilicity and other structural properties in drug design. In *Advances in Drug Research*; Testa, B., Ed.; Academic Press: London, 1987; Vol. 16, pp 87–225.
(21) Taft, R. W.; Abraham, M. H.; Doherty, R. M.; Kamlet, M. J. The molecular properties governing solubilities of organic nonelectrolytes in water. *Nature* **1985**, *313*, 384–386.
(22) El Tayar, N.; Tsai, R.-S.; Testa, B.; Carrupt, P.-A.; Leo, A. Partitioning of solutes in different solvent systems and the contribution of hydrogen-bonding capacity. *J. Pharm. Sci.* **1991**, *80*, 590–598.
(23) El Tayar, N.; Testa, B.; Carrupt, P.-A. Polar intermolecular interactions encoded in partition coefficients: An indirect estimation of hydrogen-bond parameters of polyfunctional solutes. *J. Phys. Chem.* **1992**, *96*, 1456–1461.
(24) El Tayar, N.; Tsai, R.-S.; Vallat, P.; Altomare, C.; Testa, B. Measurement of partition coefficients by various centrifugal partition chromatographic techniques: A comparative evaluation. *J. Chromatogr.* **1991**, *556*, 181–194.
(25) Vallat, P. Ph.D. Thesis, University of Lausanne, 1992.
(26) Hansch, C.; Leo, A. The Pomona College Medicinal Chemistry Project, Pomona College, Claremont, CA 91711.
(27) Gaillard, P.; Carrupt, P.-A.; Testa, B. Molecular lipophilicity potential, a tool in 3D-QSAR. *J. Comput. Aided Mol. Des.*, in press.
(28) Richards, N. G. J.; Williams, P. B.; Tute, M. S. Empirical methods for computing molecular partition coefficients: II. Inclusion of conformational flexibility within fragment-based approach. *Int. J. Quantum Chem.* **1992**, *44*, 219–233.
(29) Carrupt, P.-A.; Testa, B.; Bechalany, A.; El Tayar, N.; Descas, P.; Perrissoud, D. Morphine 6-glucuronide and morphine 3-glucuronide as molecular chameleons with unexpected lipophilicity. *J. Med. Chem.* **1991**, *34*, 1272–1275.
(30) Mierke, D. F.; Kessler, H. Molecular dynamics with dimethyl sulfoxide as a solvent. Conformation of a cyclic hexapeptide. *J. Am. Chem. Soc.* **1991**, *113*, 9466–9470.
(31) Stroup, A. N.; Rockwell, A. L.; Gierasch, L. M. Solution conformation of two flexible cyclic pentapeptides: cyclo(Gly-Pro-D-Phe-Gly-Ala) and cyclo(Gly-Pro-D-Phe-Gly-Val). *Biopolymers* **1992**, *32*, 1713–1725.
(32) Jackson, M.; Mantsch, H. H. Conformation of the peptide hormone somatostatin in aqueous solution and organic solvents. *Vib. Spectrosc.* **1992**, *3*, 323–326.
(33) Rizo, J.; Dhingra, M. M.; Gierasch, L M. Peptide models for reverse turns. The role of asparagine in the i position of a β turn. In *Molecular Conformation and Biological Interactions*; Balaram, P., Ramaseshan, S., Eds.; Indian Academy of Science: Bangalore, 1991; pp 469–496.
(34) Hsu, V. L.; Heald, S. L.; Harding, M. W.; Handschumacher, R. E.; Armitage, I. M. Structural elements pertinent to the interaction of cyclosporin A with its specific receptor protein, cyclophilin. *Biochem. Pharmacol.* **1990**, *40*, 131–140.
(35) Ko, S. Y.; Dalvit, C. Conformation of cyclosporin A in polar solvents. *Int. J. Peptide Protein Res.* **1992**, *40*, 380–382.
(36) Mark, A. E.; van Gunsteren, W. F.; Berendsen, H. J. C. Calculation of relative free energy via indirect pathways, *J. Chem. Phys.* **1991**, *94*, 3808–3816.

(37) Kâck, M.; Müller, G.; Kessler, H. Structure-activity relationship of cyclosporin A using dynamic forcing. In *Proceeding of XXII European Peptide Symposium*; Schneider, C. H., Eberle, A. N., Eds.; ESCOM Science Publishers: Leiden, 1993; pp 511–512.
(38) Thériault, Y.; Logan, T. M.; Meadows, R.; Yu, L.; Olejniczak, E. T.; Holzman, T. F.; Simmer, R. L.; Fesik, S. W. Solution structure of the cyclosporin A/cyclophilin complex by NMR. *Nature* **1993**, *361*, 88–91.
(39) Hermans, J.; Berendsen, H. J. C.; van Gunsteren, W. F.; Postma, J. P. M. A consistent empirical potential for water-protein interactions. *Biopolymers* **1984**, *23*, 1513–1518.
(40) van Gunsteren, W. F.; Berendsen, H. J. C. Groningen molecular simulation (GROMOS) library manual. *Biomos*, Nijenborgh 16, Groningen, The Netherland, 1987.
(41) Ryckaert, J.-P.; Ciccotti, G.; Berendsen, H. J. C. Numerical integration of the cartesian equations of motion of a system with constraints: Molecular dynamics of *n*-alkane. *J. Comput. Phys.* **1977**, *23*, 327–341.
(42) Berendsen, H. J. C.; Postma, J. P. M. van Gunsteren, W. F.; Hermans, J. Interaction models for water in relation to protein hydration. In *Intermolecular Forces*; Pullman, B., Ed.; Dordrecht: Holland, 1981; pp 331–342.
(43) Rebertus, D. W.; Berne, B. J.; Chandler, D. Molecular dynamics and Monte Carlo studies of solvent effects on the conformational equilibria of n-butane in CCl_4. *J. Chem. Phys.* **1979**, *70*, 3395–3400.
(44) Berendsen, H. J. C.; Postma, J. P. M.; van Gunsteren, W. F.; DiNola, A.; Haak, J. R. Molecular dynamics with coupling to an external bath. *J. Chem. Phys.* **1984**, *81*, 3684–3690.